

Research Article

Quantitative Comparison of Osteoconduction between Porous Apatite and Wollastonite-Containing Glass-Ceramics with 5 Different Pore Sizes

T. Saito,¹ M. Takemoto,¹ S. Fujibayashi,¹ M. Neo,¹ T. Murakami,² F. Miyaji,² and T. Nakamura¹

¹Department of Orthopaedic Surgery, Graduate School of Medicine, Kyoto University, Shogoin, Kawahara-cho 54, Sakyo-ku, Kyoto 606-8507, Japan

²Japan Medical Materials Corporation Uemura Nissei Bldg. 9F 3-3-31 Miyahara, Yodogawa-ku, Osaka 532-0003, Japan
Address correspondence to T. Nakamura, ntaka@kuhp.kyoto-u.ac.jp

Received 14 January 2011; Accepted 3 February 2011

Abstract Control of the porous morphology and physicochemical characteristics of ceramics is important for osteoconduction. In this study, we determined the influence of the porous structure of glass-ceramics that contain apatite and wollastonite (GC-AW) on osteoconduction. For this purpose, we prepared GC-AW cylinders (6×15 mm) with 5 different pore structures [macropore size, interconnecting pore size, and presence of micropores (pore size, approximately $1 \mu\text{m}$) for each material were as follows. Material 1000G: $800 \mu\text{m}$, $150\text{--}200 \mu\text{m}$, \pm ; material 1000S: $800 \mu\text{m}$, $175 \mu\text{m}$, $-$; material 300G: $250 \mu\text{m}$, $20 \mu\text{m}$, and $++$; Material 300S: $250 \mu\text{m}$, $20 \mu\text{m}$, $+$; and 200S: $200 \mu\text{m}$, $50\text{--}80 \mu\text{m}$, $-$]. To evaluate osteoconduction *in vivo*, these materials were implanted into holes (6 mm diameter) made in rabbit femoral condyles. The percentage of bone ingrowth area significantly increased in the case of 300G, 300S, and 200S at 6 and 12 weeks. At 3 weeks after implantation, the rate of bone ingrowth was faster when 1000G, 1000S, and 200S were used than when 300G and 300S were used. These results suggest that GC-AW with a pore size of $800 \mu\text{m}$ is unsuitable for bone growth, and rapid osteoconduction can be achieved at interconnecting pore sizes exceeding $50 \mu\text{m}$. Further, micropores may not be important for osteoconduction in the case of highly bioactive materials such as GC-AW.

Keywords glass; apatite; wollastonite; osteoconduction; vivo

1 Introduction

Glass-ceramics that contain apatite and wollastonite (GC-AW) have been widely used in clinical applications because of their high bioactivity [1]. In 2004, Ohsawa et al. described the excellent osteoconductive properties and material absorption abilities of commercially available GC-AW porous bodies [2]. This study aims to determine

the influence of the porous structure of GC-AW by using GC-AW with 5 different pore sizes.

2 Materials and methods

2.1 Preparation of materials

Porous GC-AW was prepared as follows. First, glass powder composed of 4.6% MgO, 44.7% CaO, 34.0% SiO₂, 16.2% P₂O₅, and 0.5% CaF was prepared. The glass powder and polymeric beads were mixed with polyvinyl-alcohol solution, solidified, and dried at 60 °C. Two types of polymeric beads were used as spacer particles, namely, polymethylmethacrylate beads with a particle size of $300 \mu\text{m}$ and expanded polystyrene beads with a particle size of $1000 \mu\text{m}$. The green compacts were heated to 580 °C to remove the polymeric beads and polyvinyl-alcohol and then sintered at 1050 °C in air. In order to change the microstructure of the porous bodies, they were heated at 2 different rates (G: 0.1 °C/min, S: 5 °C/min) in the temperature range of 580 °C to 800 °C, which includes the glass transition temperature. We designated the resultant 4 materials on the basis of the size of the spacer particles and heating rates as 1000G, 1000S, 300G, and 300S. The sintered porous bodies were cut into $\phi 6 \times 15$ mm rods. Additionally, conventional GC-AW with a porosity of 70% and mean pore size of $200 \mu\text{m}$ was prepared (200S) [2]. The characteristics of the 5 types of implants are provided in Table 1.

2.2 Assessment of the morphology of porous GC-AW

The pore structure of the porous GC-AW was examined using a micro focus X-ray computed tomography system (micro-CT; SMX-100CT-SV3, Shimadzu Co., Japan). Distribution of interpore connections was determined on the basis of the penetration of Hg in an evacuated porosimeter (AutoPore IV9520; Shimadzu Co., Ltd., Kyoto, Japan).

	1000G	1000S	300G	300S	200S
Micropores	+	–	++	+	–
Interconnecting pore size (μm)	175	175	20	20	50–80
Macropore size (μm)	800	800	250	250	200
Porosity (%)	78.3	74.7	79.1	75.2	71.1

Table 1: Average pore diameter, porosity, and presence of microporosity.

To observe the inner pores, fractured porous AW was analyzed using scanning electron microscopy (SEM; S-4700; Hitachi Ltd., Tokyo, Japan).

2.3 Animal experiments

To evaluate the osteoconductive ability *in vivo*, these samples were implanted into the femur metaphyses of 50 mature male Japanese white rabbits weighing 3.0–3.5 kg. The rabbits were sacrificed at 3, 6, and 12 weeks after implantation. This animal study was approved by the Animal Research Committee, Graduate School of Medicine, Kyoto University, Japan.

After the animals were sacrificed, the implants were removed, fixed in 10% phosphate-buffered formalin, and individually dehydrated in serial concentrations of ethanol. The specimens were then embedded in polyester resin, cut into sections of 80 μm thickness, and stained with Stevenel's blue and Van Gieson's picrofuchsin. A thorough microscopic analysis of the histological slides was performed using transmitted light microscopy.

To evaluate the bone ingrowth speed, we measured the depth of the new bone from the periphery of the implant. The rate of the bone ingrowth area (%) was measured on a personal computer using Adobe Photoshop CS3 and ImageJ (NIH). The rate of the bone ingrowth area was defined as the fraction of the bone area within the porous area available for bone ingrowth. Two sections surrounded by cancellous bone of either the medial or lateral condyles were examined in the case of each implant. Thus, 8 slices were analyzed for each type of implant at each implantation time. The bone area in the material was measured at 6 and 12 weeks after implantation, and the depth of bone ingrowth within the material was measured at 3 weeks. The significance of the difference in the degree was analyzed by analysis of variance (ANOVA).

3 Results

3.1 Analysis of structure and morphology

Micro-CT and 3D reconstruction image analyses revealed the 3D interconnectivity of the porous structures of all the materials. The pore diameter of the macroporous structures,

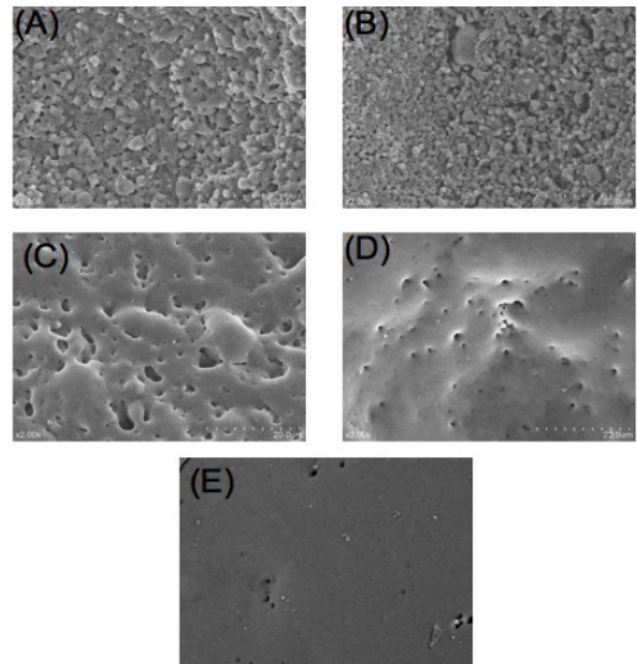


Figure 1: Presence of micropores in SEM images of (A) 300G, (B) 300S, (C) 1000G, (D) 1000S, and (E) 200S.

the diameter of interpore connections, and the total porosity were determined by mercury porosimeter and micro-CT analyses (Table 1).

Micropores (pore size, around 1 μm) were identified in the SEM image (Figure 1). These findings were compatible with the findings of mercury porosimeter analysis.

3.2 Bone ingrowth speed

In the case of 1000G, 1000S, and 200S, the bone ingrowth extended almost to the central section of the material (2.96 ± 0.04 , 2.92 ± 0.08 , and 2.90 ± 0.06 mm, respectively) at 3 weeks after implantation. In the case of 300G and 300S, the bone ingrowth extended up to one-third of the circle (1.34 ± 0.09 and 1.24 ± 0.11 mm, respectively). The rate of bone ingrowth was higher when 1000G, 1000S, and 200S were used than when 300G and 300S were used ($P < 0.01$).

3.3 Histological findings and analysis of bone ingrowth area

Microscopic analysis revealed that new bone penetration extended throughout the central zones of all materials at 6 weeks. Vascular networks were well established and bone marrow had penetrated throughout the central zone; furthermore, the bone had a more mature, organized, lamellar structure at 6 weeks (Figure 2).

The percentage of bone ingrowth area significantly increased in the case of 300G, 300S, and 200S at 6 and 12 weeks after implantation compared to that in the case of 1000G and 1000S ($P < 0.05$) (Figure 3).

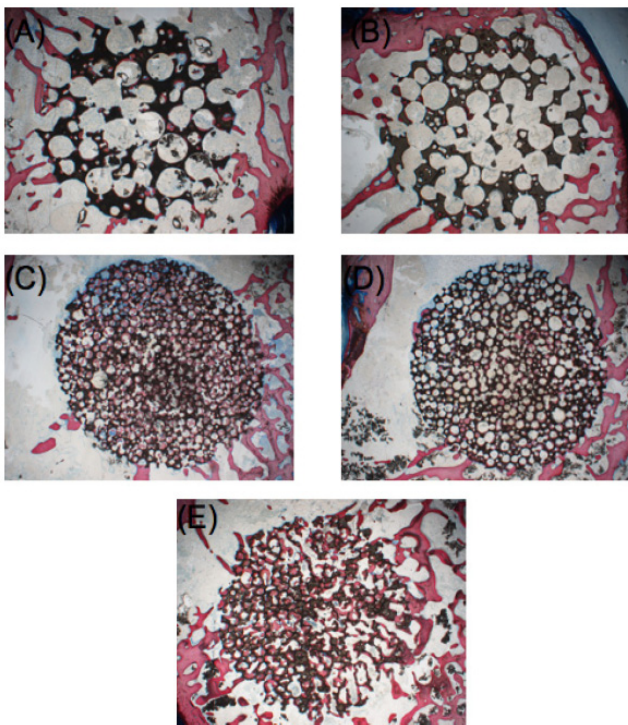


Figure 2: Microscopic images after staining with Stevenel's blue and Van Gieson's picrofuchsin at 6 weeks. (A) 1000G, (B) 1000S, (C) 300G, (D) 300S, and (E) 200S.

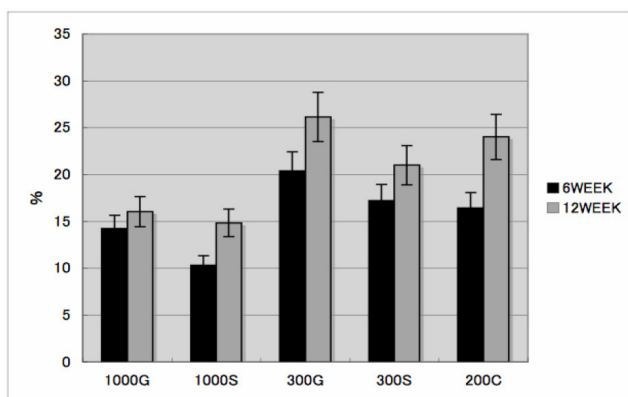


Figure 3: Percentage of bone ingrowth area at 6 and 12 weeks.

Absorption of all materials was clearly visible, especially in the case of 300G and 200S (Figure 2).

4 Discussion and conclusion

Porous bioactive ceramics and glass implants have been widely used in the clinical setting as a bone substitute. In the case of these materials, 2 important factors affect osteoconduction, namely, their physicochemical characteristics (e.g., hydroxyapatite, glass, and TCP) and porous topography.

Porous topography includes the macropore, interconnective pore, and micropore sizes as well as pore interconnectivity. In scientific literature, determination of the optimum pore size has been the topic of numerous studies. Generally, a macropore size of 50–800 μm and an interconnection pore size of 50–100 μm are considered adequate [3]. It is still controversial whether or not micropores are essential for osteoconduction. Our results suggest that GC-AW with a pore size of 800 μm is unsuitable for bone growth, and rapid osteoconduction can be achieved at interconnecting pore sizes exceeding 50 μm . These results are consistent with those of other reports. The interconnecting pore sizes in the case of 300G and 300S are approximately 20 μm , and this size maybe too small for osteoconduction; however, GC-AW is a resorptive material, and its interconnecting pores may expand with the implantation period. As for the micropores, they may not be important for osteoconduction in the case of highly bioactive materials like GC-AW.

References

- [1] T. Nakamura, T. Yamamuro, S. Higashi, T. Kokubo, and S. Itoo, *A new glass-ceramic for bone replacement: evaluation of its bonding to bone tissue*, *J Biomed Mater Res*, 19 (1985), 685–698.
- [2] K. Ohsawa, M. Neo, T. Okamoto, J. Tamura, and T. Nakamura, *In vivo absorption of porous apatite- and wollastonite-containing glass-ceramic*, *J Mater Sci*, 15 (2004), 859–864.
- [3] M. C. von Doernberg, B. von Rechenberg, M. Bohner, S. Grünenfelder, G. H. van Lenthe, R. Müller, et al., *In vivo behavior of calcium phosphate scaffolds with four different pore sizes*, *Biomaterials*, 27 (2006), 5186–5198.